Received: 28 April 2021 | Revised: 26 November 2021 | Accepted: 17 December 2021

DOI: 10.1096/fj.202100707R

THE FASEB JOURNAL

RESEARCH ARTICLE

Time-restricted feeding during the inactive phase abolishes the daily rhythm in mitochondrial respiration in rat skeletal muscle

Paul de Goede[1,2] | **Rob C. I. Wüst**[3,4] | **Bauke V. Schomakers**[3,5] | **Simone Denis**[3] | **Frédéric M. Vaz**[3,5] | **Mia L. Pras-Raves**[3,5] | **Michel van Weeghel**[3,5] | **Chun-Xia Yi**[1,6] | **Andries Kalsbeek**[1,2,6] | **Riekelt H. Houtkooper**[3]

[1]Laboratory of Endocrinology, Amsterdam Gastroenterology, Endocrinology, and Metabolism, Amsterdam University Medical Center, University of Amsterdam, Amsterdam, The Netherlands

[2]Hypothalamic Integration Mechanisms Group, Netherlands Institute for Neuroscience (NIN), an Institute of the Royal Netherlands Academy of Arts and Sciences, Amsterdam, The Netherlands

[3]Laboratory Genetic Metabolic Diseases, Amsterdam Gastroenterology, Endocrinology, and Metabolism, Amsterdam Cardiovascular Sciences, Amsterdam University Medical Center, University of Amsterdam, Amsterdam, The Netherlands

[4]Laboratory for Myology, Department of Human Movement Sciences, Faculty of Behavioural and Movement Sciences, Vrije Universiteit Amsterdam, Amsterdam, The Netherlands

[5]Core Facility Metabolomics, Amsterdam University Medical Center, University of Amsterdam, Amsterdam, The Netherlands

[6]Department of Endocrinology and Metabolism, Amsterdam University Medical Center, University of Amsterdam, Amsterdam, The Netherlands

Correspondence
Riekelt H. Houtkooper, Laboratory Genetic Metabolic Diseases, Amsterdam UMC, University of Amsterdam, Amsterdam Gastroenterology, Endocrinology, and Metabolism, Amsterdam Cardiovascular Sciences, Amsterdam, The Netherlands.
Email: r.h.houtkooper@amsterdamumc.nl

Funding information
P. de Goede was funded by a ZonMW TOP grant (#91214047)

Abstract

Shift-workers show an increased incidence of type 2 diabetes mellitus (T2DM). A possible mechanism is the disruption of the circadian timing of glucose homeostasis. Skeletal muscle mitochondrial function is modulated by the molecular clock. We used time-restricted feeding (TRF) during the inactive phase to investigate how mistimed feeding affects muscle mitochondrial metabolism. Rats on an *ad libitum* (AL) diet were compared to those that could eat only during the light (inactive) or dark (active) phase. Mitochondrial respiration, metabolic gene expressions, and metabolite concentrations were determined in the *soleus* muscle. Rats on AL feeding or dark-fed TRF showed a clear daily rhythm in muscle mitochondrial respiration. This rhythm in mitochondrial oxidative phosphorylation capacity was abolished in light-fed TRF animals and overall 24h respiration was lower. The expression of several genes involved in mitochondrial biogenesis and the fission/fusion machinery was altered in light-fed animals. Metabolomics analysis indicated that light-fed animals had lost rhythmic levels of α-ketoglutarate and

Abbreviations: AL, *ad libitum*; L/D, light/dark; OXPHOS, oxidative phosphorylation; RER, respiratory exchange ratio; T2DM, type 2 diabetes mellitus; TCA, tricarboxylic acid cycle; TRF, time-restricted feeding; ZT, Zeitgeber timepoint.

Full names of all the tested genes and lipid species can be found in Tables S1 and S6, respectively.

citric acid. Contrastingly, lipidomics showed that light-fed animals abundantly gained rhythmicity in levels of triglycerides. Furthermore, while the RER shifted entirely with the food intake in the light-fed animals, many measured metabolic parameters (e.g., activity and mitochondrial respiration) did not strictly align with the shifted timing of food intake, resulting in a mismatch between expected metabolic supply/demand (as dictated by the circadian timing system and light/dark-cycle) and the actual metabolic supply/demand (as dictated by the timing of food intake). These data suggest that shift-work impairs mitochondrial metabolism and causes metabolic inflexibility, which can predispose to T2DM.

KEYWORDS

lipidomics, metabolomics, mitochondrial respiration, *soleus* muscle, time-restricted feeding

1 | INTRODUCTION

The biological clock controls a wide variety of metabolic processes, on a systemic as well as a cellular level. This endogenous timing system enables organisms to anticipate predictable daily changes in the environment, such as food availability and prepares cellular metabolism for appropriate energy substrate selection, for example, carbohydrates during the active (awake) period and lipids during the inactive (sleep) period. Indeed, on a cellular level, many aspects of metabolism are under circadian control, including mRNA transcripts, protein levels, post-translational modifications as well as metabolites.[1-3] For example, 43% of all protein-coding genes were rhythmically expressed in at least one mouse organ, with 3%–14% of all transcripts being rhythmic in the individual organs.[3] Additionally, in the mouse liver, ~50% of all metabolites, including several metabolites of the tricarboxylic acid cycle (TCA) cycle, were rhythmically fluctuating.[1]

Disruption of this temporal balance between energy supply and energy demand is suspected to lead to various metabolic diseases, including type 2 diabetes mellitus (T2DM). For instance, epidemiological evidence indicates that night shift workers are at an increased risk of developing T2DM, most likely because of the frequent disturbance of their biological clock by having nocturnal light exposure, and being active and eating at the "wrong" time of day[4,5] (reviewed in Ref. [6]).

T2DM is characterized by augmented endogenous glucose production as well as lower glucose uptake as a result of insulin resistance. The full complexity underlying the pathophysiology of insulin resistance remains incompletely understood, but one possible contributing factor is a disturbance in mitochondrial substrate metabolism,[7-13] as T2DM patients have impaired skeletal muscle mitochondrial function.[14-18] Skeletal muscle is an important organ for glucose uptake as it comprises up to 50% of total body mass in mammals and is considered to be the primary target for insulin-stimulated glucose uptake.[19-22]

Several "-omics" approaches demonstrated that metabolic gene expression in skeletal muscle shows daily rhythms, both in humans and rodents, with transcripts for mitochondrial activity clustered in the afternoon in humans and in either of two peaks in the dark and light phase in mice.[3,23,24,25,26,27] Skeletal muscle mitochondrial dynamics and respiration are also under the control of the biological clock (reviewed in Refs. [28-30]). However, it is currently unknown whether the mitochondrial respiration rhythm in muscle fibers can be enhanced and/or disturbed through methods other than interrupting gene expression (e.g., altered feeding behavior). Therefore, in the current study, we used high-resolution respirometry, combined with gene expression, metabolomics, and lipidomics to study skeletal muscle mitochondrial metabolism in rats with a normal *ad libitum* (AL) diet. Using time-restricted feeding (TRF) during the light phase as a model for shift work, we investigated how eating at the "wrong" time of the day affects the daily rhythm in mitochondrial respiration and metabolite profiles.

2 | MATERIALS AND METHODS

2.1 | Animals and housing

Ninety-six adult male Wistar WU rats (8 weeks old; 253 ± 14 g upon the start of the experiment, Charles River) were used for the current experiments. All rats were housed under 12:12=light:dark conditions in a controlled environment of ~21°C during the entire experiment. Zeitgeber Time 0 (ZT0) was defined as the time of lights on and ZT12 as the time of lights off. All animals had AL access to tap water during the entire experiment. At the start of the experiment, animals were randomly assigned to one of three

feeding groups: AL fed, dark-fed TRF, or light-fed TRF. *Ad libitum* fed animals had AL access to food 24 h/day, TRF animals had also AL access to food, but only for 10 h during either the light or dark phase. Dark-fed animals had access to food from ZT13-23, while light-fed animals had access to food from ZT1-11 (Figure 1A). Bodyweight of the animals was measured weekly. Food intake was measured after the animals were habituated to the TRF protocol either in the third or fourth experimental week (7 days average). All experiments were approved by the Dutch government and performed in accordance with the guidelines on animal experimentation of the Netherlands Institute for Neuroscience (License number: AVD801002016693/IVD 576).

2.2 | Metabolic cages

Metabolic PhenoCages (TSE systems) were used to assess metabolic parameters such as locomotor activity, food intake, and the respiratory exchange ratio (RER) in a separate group of experimental animals. Eight rats were placed in these metabolic cages and remained inside these cages for 4 weeks (4 days AL feeding and 3.5 weeks of TRF in either the light (n = 4) or dark (n = 4) phase). Cages were cleaned twice a week. Data shown are from the last 2 days of AL feeding and the last 3 days of the TRF feeding phase.

2.3 | Body temperature loggers

To assess body temperature, loggers (DST nano-T, STAR ODDI) were placed subcutaneously in another subset of animals (n = 5), while the animals were anesthetized. Temperature loggers were placed at the lumbar back region to prevent interference with brown adipose tissue activity. After recovery from the surgery, the temperature loggers were measured continuously until the end of the experiment with one sampling point every 15 minutes. Each animal was first measured for 3 days during AL feeding and subsequently during TRF to either the light (n = 3) or dark (n = 2) phase for 3.5 weeks.

2.4 | Muscle tissue preparation

After 4 weeks of TRF (between 3.5 and 4.5 weeks) animals were sacrificed at ZT3, 7, 15, or 19. As only one animal could be sacrificed per measurement session, the timing of sacrifice was highly standardized (1-minute deviation from the actual ZT). Furthermore, all further steps involving tissue preparation up until the start of the oxygen consumption measurement were highly standardized in their timing to minimize variation between the measurements.

2.4.1 | Mitochondrial respiration

After sacrifice, the left *soleus* muscle was dissected, snap-frozen in liquid nitrogen, and stored at -80°C for later analysis. The middle part of the right *soleus* muscle was excised, and stored in respiration solution B (2.8 mM CaK_2EGTA, 7.2 mM K_2EGTA, 5.8 mM ATP, 6.6 mM magnesium chloride, 20 mM taurine, 15 mM phosphocreatine, 20 mM imidazole, 0.5 mM DTT, and 50 mM MES (pH 7.1)) on ice, and further separated into fiber bundles (3–10 fibers) under a light microscope. Next, saponin (50 μg/ml) was added for 30 minutes to permeabilize the outer cellular membrane. Subsequently, the muscle fibers were washed twice with Mir05 (0.5 mM EGTA, 3 mM magnesium chloride, 60 mM K-lactobionate, 20 mM taurine, 10 mM potassium dihydrogen phosphate, 20 mM HEPES, 110 mM sucrose, and 1 g/L fatty acid-free BSA (pH 7.1)), quickly blotted dry and weighed before placing them in a respirometer (O2k, Oroboros Instruments, Innsbruck, Austria). The following substrate-uncoupler-inhibition-titration (SUIT) protocol was used for all measurements, similar to the previous studies.[31,32] To start, background respiration was measured for 10–15 minutes. Next, leak respiration was measured by the addition of sodium glutamate (10 mM), sodium malate (0.5 mM), and sodium pyruvate (5 mM). Maximal complex I-stimulated respiration with NADH producing substrates was measured after the addition of 2.5 mM ADP. The integrity of the mitochondrial membrane was tested by a lack of stimulation by 10 μM cytochrome c. Maximal oxidative phosphorylation (OXPHOS) was measured by subsequent convergent input of electrons via complex I and II after adding 10mM succinate. Carbonylcyanide-4-(trifluoromethoxy)-phenylhydrazone (FCCP) was stepwise (0.01 mM steps) titrated until maximal uncoupled respiration was reached. Subsequently, 0.5 μM rotenone was added to block mitochondrial complex I. Lastly, 2.5 μM antimycin A was used to block all electron transport-related respiration and this oxygen consumption level was used to subtract from all values. Chamber oxygen levels were maintained above 300 nM to prevent oxygen being limited. Respiration was measured in duplo for each animal at the same time.

2.5 | Gene expression profiles

2.5.1 | RNA isolation

Soleus muscle tissue was kept on dry ice to preserve mRNA integrity during mechanical homogenization. RNA isolation was performed using the ISOLATE II RNA Mini Kit (Bioline). RNA was eluted from the spin column using 40 μl of H_2O after which RNA

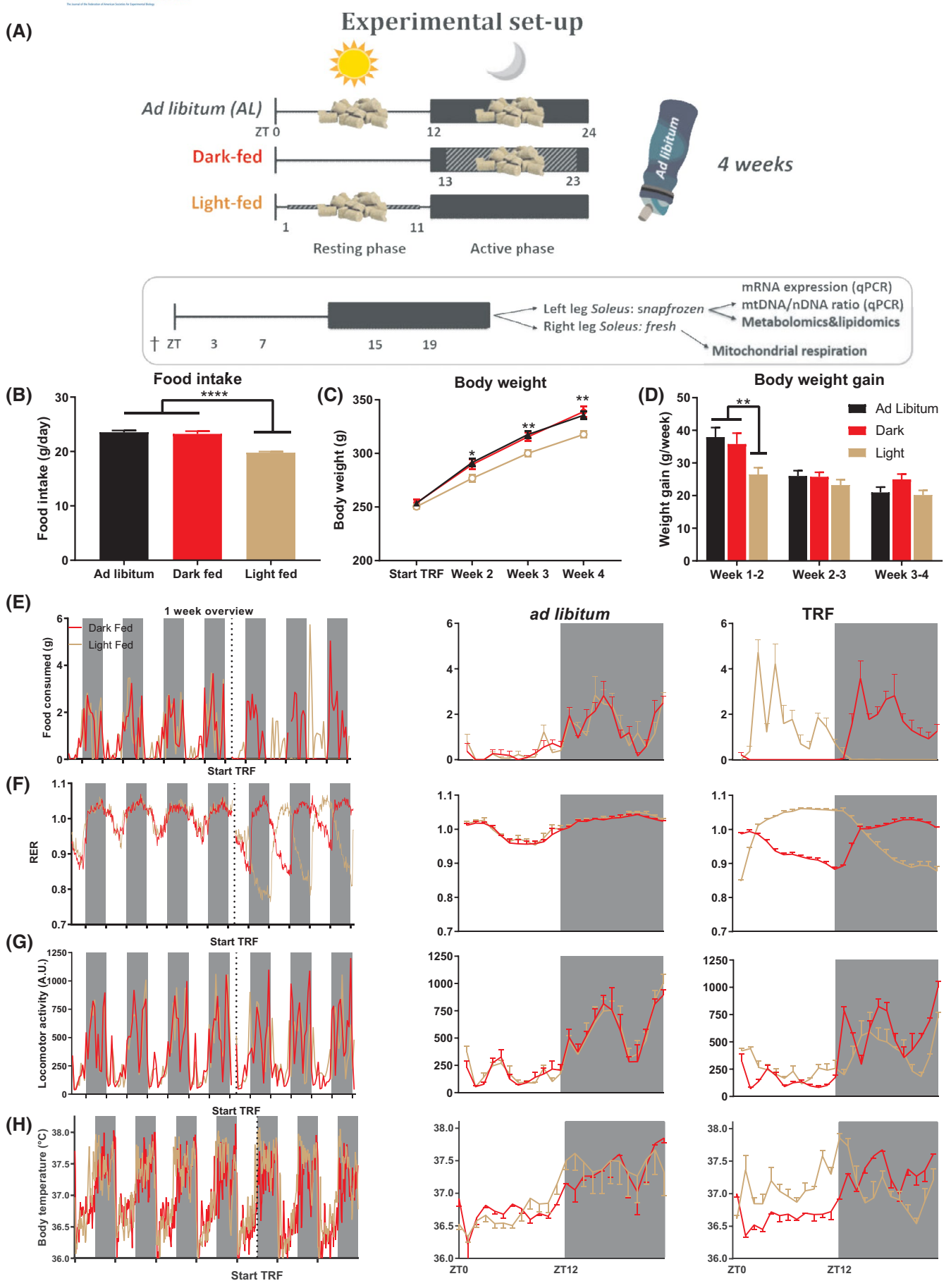

FIGURE 1 Legend on next page

FIGURE 1 Experimental design and basic physiological measures of the three experimental groups. (A) Schematic representation of the experimental procedure. Depicted are the three different TRF groups, the time periods they can eat, and the time points of sacrifice. (B) Daily food intake in the final week of the TRF protocol was significantly lower for the light-fed animals as compared to the *ad libitum* and dark-fed group (average food intake of 7 days per animal). (C) Growth curve of the animals during the experiments. Light-fed animals had significantly lower body weights as compared to the *ad libitum* and dark-fed group starting from the second week of the TRF protocol. (D) Weekly body weight gain of the animals. Only in the first week of the experimental procedure the light-fed animals grew significantly less. $N = 32$ per experimental group. (E–H) Overview of the metabolic parameters of the animals: food intake (E), RER (F), locomotor activity (G), and subcutaneous body temperature (H). While in the metabolic cages or with body temperature loggers implanted, animals transitioned from the *ad libitum* feeding condition to their assigned feeding regimen (left figures). The middle figures show the hourly profile of the metabolic measures during the *ad libitum* feeding phase (3-day average). The right figures show the hourly profile of the metabolic measures during the 4th week of the TRF feeding phase (3-day average). Locomotor activity is presented as arbitrary units (AU). Shaded areas represent the dark phase. $n = 4$ per experimental group for the parameters of the metabolic cages (E–G) and $n = 2$–3 per experimental group for the subcutaneous body temperature (H). Table 1 summarizes the main statistical findings for the metabolic parameters displayed in E–H. Note that for E–H the figures to the left show data from one full week, that is, 4 days of *ad libitum* feeding and the first 3 days of the TRF phase, the *ad libitum*- and TRF-phase being separated by a dashed line. This means the TRF data in the left figures are different from those in the right figures, as the former displays the first 3 days of the TRF period, whereas the latter are summaries of the 4th week of the TRF period. $^{*}p < .05$, $^{**}p < .01$, $^{****}p < .0001$ using Tukey's post hoc tests

concentration and quality of the RNA were determined using a DS-11 (DeNovix) spectrophotometer and using the Agilent 2100 Bioanalyzer (Agilent Technologies), respectively. Although RNA integrity number (RIN) values above 5 were considered acceptable, all samples had a RIN above 8.

2.5.2 | cDNA synthesis

Three hundred and fifty ng of RNA was used as input for the cDNA synthesis. The Transcriptor First Strand cDNA synthesis kit (Roche) was used with oligo-dT primers and several additional samples without reverse transcriptase (-RT) were used as negative controls to check for genomic DNA contamination during the RT-qPCRs. RT-PCRs were run using an UNO-Thermoblock (Biometra) (30 min at 55°C, 5 min at 85°C).

2.5.3 | qPCR

One to 19 (1:19) diluted cDNA was used for all qPCRs to detect daily gene expression profiles. Expression levels of all genes were standardized by dividing over the geometric mean of three reference genes: RSP S18, β-actin, and Cyclophilin. This geometric mean showed no significant effects of time of day (*ZT)* or feeding condition (*TRF*) nor for the *ZT* × *TRF* interaction. RT-qPCR was performed using a LightCycler 480 (Roche). Expression levels were calculated using dedicated software for linear regression of qPCR data (LinRegPCR). All primers used are listed in Table S1. Melting curves of the RT-qPCR and fragment length of the DNA amplicons were inspected as a means of quality control.

2.6 | mtDNA/nDNA isolation and quantification

DNA isolation was performed using the DNA mini isolation kit (Qiagen) according to the manufacturer's guidelines. DNA was eluted from the spin column using 200 µl of H_2O after which DNA concentration was determined using a DS-11 (DeNovix). For the RT-qPCR of the mtDNA/nDNA ratio and the subsequent analysis and quality control, similar procedures were used for the gene expression described above (Section 2.5.3). However, for the mtDNA/nDNA ratio qPCRs, an input of 6ng per reaction well was used. Primers used for the nuclear and mitochondrial DNA fragments are listed in Table S1.

2.7 | Citrate synthase measurements

Tissue samples (1–2 mg wet weight) were disrupted in 100 mM Tris/HCl-KCl buffer, pH 7.6 and 1 g/L Triton X-100 using a TissueLyser II (Qiagen) for 1 min at a frequency of 30 times/sec, followed by sonication (twice at 8-watt output, 40 J, on ice). The homogenates were centrifuged for 5 minutes at 500 g. Protein concentration was determined in the supernatant using the BCA method. The homogenates were diluted to 0.3 mg/ml. Citrate synthase (CS) was measured spectrophotometrically at 412nm by the formation of free CoA using 5,5'-Dithio-Bis (2-Nitrobenzoic Acid) (DTNB).[33] CS was assayed in 250 µl of 125 mM Tris/HCl-KCl buffer, pH 7.6, containing (final concentrations) DTNB (0.1 mM), acetyl-CoA (200 µM), Triton X-100 (1 g/L) and oxaloacetate (200 µM). The addition of oxaloacetate was used to start the enzymatic reaction after a preincubation

period of 5 min. The reduction of DTNB was followed in time on a CobasFara centrifugal analyzer (Roche) at 412 nm, with the use of a molar extinction coefficient of 13 600 L/mol/cm.

2.8 | Polar metabolomics and lipidomics

Metabolomics and lipidomics were performed as previously described, with minor adjustments.[34] Briefly: for each sample, approximately 5 mg of freeze-dried *soleus* muscle was added to a 2 ml Eppendorf Safe-Lock tube. Internal standards for both metabolomics and lipidomics were added, as well as solvents for a total of 500 μl water, 500 μl methanol, and 1 ml chloroform. Samples were homogenized using a stainless steel bead before centrifugation, creating a two-phase system. Polar metabolomics was performed on the top layer using a ZIC-cHILIC LC-MS platform, while lipidomics was performed on the bottom layer, using both a normal and reversed-phase LC-MS platform.

2.9 | Statistics

Rhythmicity of physiological parameters (food intake, RER, locomotion, and body temperature) was determined using SigmaPlot 14.0 (Systat Software) as this software package can take into account within-individual measures.

Rhythmicity of gene expression, metabolomics/lipidomics, and mitochondrial respiration measures was determined using the JTK_Cycle 3.0 script for non-parametric cosine regression, as this software package is best suited for independent sampling with lower temporal resolution (less than 24 time points per 24 h cycle) and can correct for the multiple comparisons problems, which is necessary when, for example, testing a multitude of gene expression profiles from the same mRNA/cDNA pool during qPCR. The JTK_Cycle script was run in RStudio (R version 3.3.3). All graphs were plotted using Graphpad Prism 7. All other statistics, including the one-way and two-way ANOVA's, were executed by Graphpad Prism 7.

3 | RESULTS

3.1 | Physiological parameters display altered rhythms upon TRF

To confirm that during the TRF phase animals showed similar metabolic phenotypes as in our previous studies, we monitored food intake and body weight and placed a subset of animals in metabolic cages to assess rhythms in metabolic parameters such as RER.[35-38] In the final week of the TRF protocol, the daily food consumption ranged between 19 and 24 g per day and was lowest for the light-fed animals, but did not significantly differ between AL fed and dark-fed animals (Figure 1B). Animals continuously gained body weight throughout the experiment (Figure 1C,D), but light-fed animals gained the least amount, likely due to the necessary adaptation to the TRF in the first week, as food intake was ~25% less in this first week compared to the AL group (data not shown). In the remainder of the experiment light-fed animals gained similar amounts of body weight as the other groups (Figure 1D), despite eating significantly less (Figure 1B). Thus, contrary to most mice studies, rats eating at the wrong time of day did not show an increased body weight, this could be due to the fact that in the current experiment the feeding period was only 10 h, instead of 12 h, or a stronger light-induced inhibition of activity and feeding behavior during the light period in rats as compared to mice. In contrast, feeding efficiency was increased in the light-fed animals and in previous experiments, we found increased adiposity in the light-fed animals.[37-39]

A subset of animals was housed in metabolic cages, first under AL (baseline) feeding conditions and subsequently under TRF conditions (4 weeks) to assess physical activity and substrate metabolism. As expected, light-fed and dark-fed animals did not eat during the dark and light phases, respectively (Figure 1E). Similar to our previous experiments, under AL conditions animals consumed most of their food in the dark phase (85%), with 61% of total food intake in the dark phase being consumed in the first half of the dark phase. Such a bimodal feeding pattern was also found during the TRF phase, with the obvious difference that the light-fed animals had their two peaks in food consumption during the light phase (Figure 1E). Light-fed animals ate slightly more during the first half of their feeding period (63% of total food intake) as compared to the dark-fed animals (56% of total food intake).

The amplitude of the daily rhythm in RER increased in animals on TRF, both for the light and dark-fed groups, especially due to a greater reliance on lipid substrate utilization during the non-feeding period (Figure 1F, Table 1). Dark-fed animals were relatively more active during the dark phase and light-fed animals were more active during the light phase (Figure 1G, Table 1), as compared to AL feeding. However, the shift in locomotor activity in the light-fed animals was clearly less pronounced than the shift in food intake, as the light/dark (L/D) ratio for locomotor activity went from 20/80 during AL feeding to 50/50 during light phase TRF. Importantly, the TRF-induced alterations in RER and locomotor activity were highly similar to those reported previously.[35,37,38]

TABLE 1 Analysis of rhythmicity of the physiological parameters from animals that went from *ad libitum* feeding (AL phase) to either dark or light phase feeding (TRF phase)

	Rhythmicity		Acrophase		Amplitude[a]	
	Light-fed (*p*-value)	Dark-fed (*p*-value)	Light-fed (ZT)	Dark-fed (ZT)	Light-fed	Dark-fed
Food intake AL phase	<.001	<.001	12.7	12.5	0.91 (g)	0.88 (g)
Food intake TRF phase	<.001	<.001	5.2	17.1	1.15 (g)	1.27 (g)
Respiratory exchange ratio (RER) AL phase	<.001	<.001	19.0	19.0	0.0379	0.0381
Respiratory exchange ratio (RER) TRF phase	<.001	<.001	8.6	20.2	0.0968	0.0640
Locomotion AL phase	<.001	<.001	18.5	17.9	273.2 (AU)	263.8 (AU)
Locomotion TRF phase	<.001	<.001	18.4	18.0	136.9 (AU)	283.7 (AU)
Body temperature AL phase	<.001	<.001	16.8	18.3	0.68 (°C)	0.43 (°C)
Body temperature TRF phase	<.001	<.001	11.1	17.7	0.26 (°C)	0.45 (°C)

[a]Rhythm amplitudes were determined by cosinor using Sigmaplot 14.

The switch from AL feeding to light phase feeding also drastically changed the daily pattern in body temperature (Figure 1H right panel, Table 1). Such a change was not observed when animals switched from AL feeding to dark phase feeding.

3.2 | Mitochondrial respiration rhythm is abolished upon light phase TRF feeding

After confirming the metabolic effects of TRF we assessed if the *soleus* muscle of rats displays rhythms in mitochondrial respiration and whether such rhythms could be altered through TRF. Mitochondrial respiration of the *soleus* muscle was determined at four timepoints along the 24-h cycle. The light-fed animals had an overall lower OXPHOS capacity, maximal uncoupled respiration, and succinate/rotenone-linked respiration compared to AL animals, with the largest differences (~30% lower) at ZT7 (Figure 2A–C). Mitochondrial respiration showed significant differences over the 24 h cycle, but no interactions of *ZT* × *TRF* were found (Figure 2A–C, Table 2). The strongest rhythmicity was found for maximal OXPHOS capacity with combined NADH-substrates and succinate in the dark-fed animals. The AL fed group showed a trend toward a time-of-day effect, but no significant time-of-day effect was found for the light-fed group. The difference between the highest and lowest maximal OXPHOS was 17% in AL and dark-fed animals, but 11% in light-fed. Similar results were obtained for the maximal uncoupled respiration. For uncoupled respiration rates, the difference between the highest and lowest rates was about 15% for the AL group, 19% for dark-fed, and only 8% for the light-fed animals. None of the groups showed any significant daily rhythmicity after inhibition of mitochondrial complex I by rotenone, although the dark-fed animals still showed a trend towards rhythmicity, suggestive of a contributing role for mitochondrial complex I in the regulation of daily rhythmicity. Together, these data indicate that enhancing the daily feeding rhythm enhances mitochondrial respiration rhythms, while disturbing the daily feeding rhythm abolishes the mitochondrial respiration rhythm and impairs the 24-h mean respiration. Additional to the potential role of complex 1 described above, likely the mitochondrial number per muscle fiber plays a role as uncoupling respiration from OXPHOS did not lead to similar respiration between the three TRF groups.

To further assess the mechanisms that drive these alterations in respiration upon manipulation of the daily feeding rhythm, we measured the number of mitochondria per muscle fiber. The relative number of mitochondria per fiber was quantified using the ratio of DNA copy numbers of a mitochondrial DNA (mtDNA) fragment divided by the copy numbers of a nuclear DNA (nDNA) fragment (Figure 2D). No significant effects were found for the time of day (*ZT*), feeding group (*TRF*), or for the interaction *ZT* × *TRF*. However, when we performed rhythmicity analysis with JTK_Cycle, we found that only in the light-fed group the mtDNA/nDNA ratio was rhythmic ($p = .0198$), which likely can be attributed to the diurnal fluctuations in mtDNA abundance and not the nDNA abundance ($p = .0248$ and $p > .9999$, respectively, JTK_Cycle, data not shown). For the AL and dark-fed groups no rhythms in mtDNA/nDNA ratio were found ($p > .9999$ for both groups). Strikingly, similar rhythmicity patterns

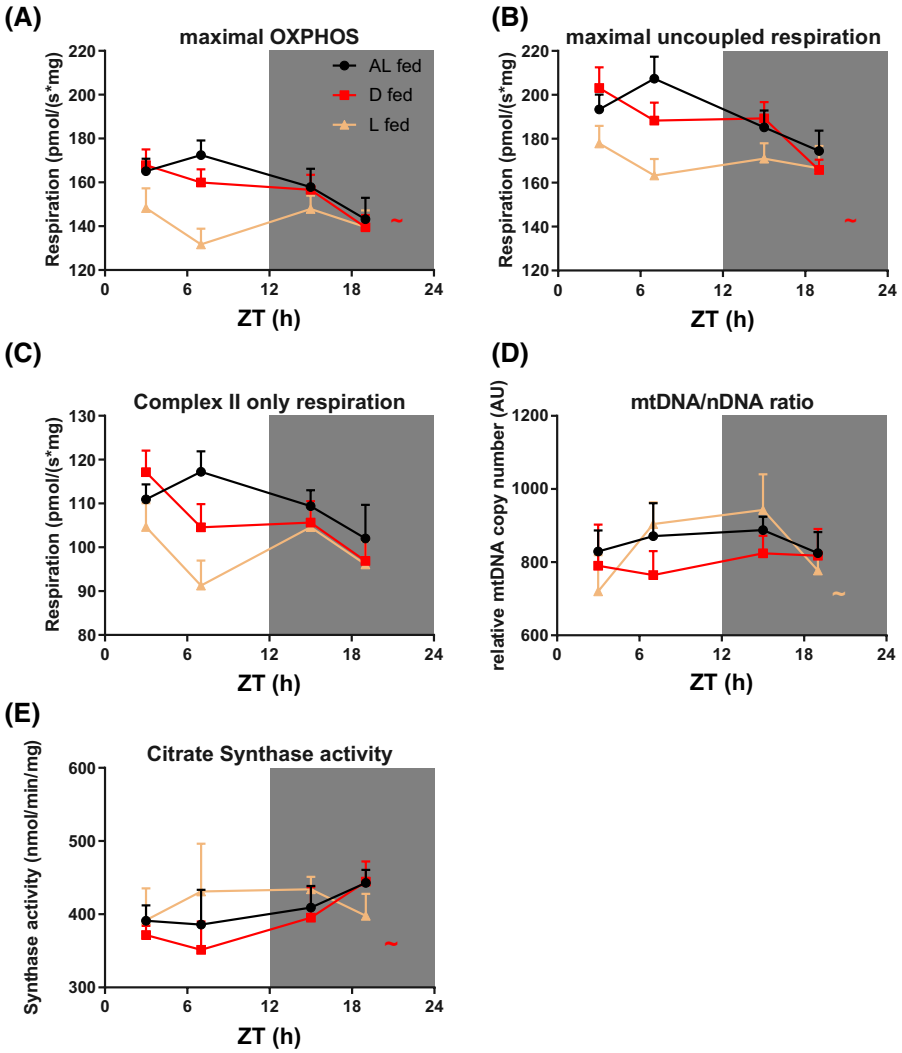

FIGURE 2 Daily profiles of the different mitochondrial respiration states and the mitochondrial abundance (mtDNA/nDNA ratio). (A) Maximal oxidative phosphorylation (OXPHOS; with pyruvate, glutamate, malate, and succinate). (B) Maximal uncoupled respiration (with FCCP). (C) Complex II only respiration (with succinate/rotenone). (D) Mitochondrial abundance (mtDNA/nDNA ratio). (E) Citrate synthase activity; Three technical replicates were measured for each biological replicate. $n = 6–8$ per experimental group per time point. Table 2 summarizes the main statistical findings for the mitochondrial respiration states and mtDNA/nDNA ratio. Color-coded "~" indicates that the (metabolic) parameter is significantly rhythmic for that TRF group as determined by JTK_Cycle ($p < .05$)

were found when we measured citrate synthase enzyme activity, which is another standard assay to reflect the mitochondrial abundance and activity (Figure 2E).

3.3 | Gene expression of some mitochondria-related genes is altered during TRF

To pinpoint the mechanisms underlying the alterations in mitochondrial respiration described above, we also measured the expression profiles of several genes that are associated with (mitochondrial) metabolism (Figure 3D–I). TRF during the light phase dampened the daily rhythmicity of the muscle clock (the core clock gene *Bmal1)* and altered the expression of several metabolic genes, including uncoupling protein 3 (*Ucp3*) and fatty acid synthase (*Fasn*). *Ucp3* expression profile was inverted with an overall lower expression in the light-fed group compared to the dark and AL-fed animals. TRF induced rhythmicity in *Fasn* expression in both the light and dark-fed groups, albeit in exact antiphase (acrophases at ZT8 and ZT20, respectively) (Figure 3A–C), which is likely explained by the food intake per se.

Also, several genes important for mitochondrial biogenesis and dynamics showed different expression profiles in the AL and the dark-fed group as compared to the light-fed group: *Ppargc1α* showed a loss of rhythm, while *Mfn1* showed a gain of rhythm. Additional genes important for mitochondrial functioning that showed altered expression in the light-fed group, included Nocturnin (*Noct*, loss of rhythm), *Sirtuin 3* (*Sirt3*, gain of rhythm), mechanistic target of rapamycin kinase (*mTOR*; gain of rhythm), and *Sarcolipin* (*Sln*, loss of rhythm).

3.4 | Metabolomics and lipidomics

3.4.1 | TRF alters rhythms in major metabolic pathway intermediates

To further characterize metabolic changes in *soleus* muscle resulting from TRF we performed polar metabolomics

TABLE 2 Summary of the two-way ANOVA of oxidative phosphorylation (OXPHOS) capacity, maximal uncoupled respiration, succinate/rotenone-linked respiration, mtDNA/nDNA ratio, and CS activity

	Two-way ANOVA *p* values			Post-hoc differences for effect of time		
Step	**ZT**	**TRF**	**TRF post-hoc test**	**TRF group**	**One-way ANOVA (ZT)**	**JTK_Cycle**
OXPHOS capacity (Figure 2A)	**0.011**	**0.002**	L < AL & D	AL	0.084	0.192
				D	**0.026**	0.091
				L	0.367	0.999
Uncoupled respiration (Figure 2B)	**0.008**	**0.001**	L < AL & D	AL	0.072	0.120
				D	**0.019**	0.091
				L	0.604	0.999
Succinate/rotenone (Figure 2C)	**0.030**	**0.015**	L < AL	AL	0.241	0.368
				D	0.072	0.322
				L	0.247	0.999
mtDNA/nDNA ratio (Figure 2D)	0.594	0.128	–	AL	0.885	0.999
				D	0.942	0.999
				L	0.172	**0.020**
Citrate synthase activity (Figure 2E)	0.680	0.626		AL	0.643	0.102
				D	0.185	**0.041**
				L	0.123	0.444

Note: Post hoc differences between groups are displayed. For the effect of time both one-way ANOVAs and cosinor analyses using JTK_Cycle were used as post-hoc test. No significant interactions (*ZT* × *TRF*) were found. Bold values correspond to *p*-values <.05.

and lipidomics. Out of 97 polar metabolites that we identified in the AL and dark-fed groups, 18% and 16% were rhythmic in the *soleus* (17 and 16 metabolites, respectively; Figure 4, Figure S1, Table S4), versus only 8% in light-fed animals (8 metabolites).

Only malate showed significant daily rhythmicity in all three groups. Coenzyme A, citric acid, and succinyl AMP (which is cleaved into both AMP and fumarate) showed significant rhythmicity in AL and dark-fed animals, whereas cis-aconitate, fumarate, and oxaloacetate trended to have a 24 h rhythm in AL and dark-fed groups ($p < .1$).

Intermediates from the pentose phosphate pathway (erythrose-4-phosphate, gluconate-6P, and ribose) were significantly rhythmic in dark-fed animals, while no intermediates were rhythmic in muscle tissue of AL or light-fed animals. In AL animals one glycolysis intermediate was found to be rhythmic (glucose), while in dark-fed animals four rhythmic glycolysis metabolites were found (fructose-6P, glucose-6P, uridine, and its precursor cytidine). Only in light-fed animals the breakdown products of both anaerobic glycolysis (lactate) and creatine phosphate metabolism (creatinine) were found to be rhythmic. Surprisingly, many of the metabolites that were significantly rhythmic in at least one of the TRF groups were amino acids and nucleic acids (Table S4).

For most metabolites overall daily (i.e., 24-h average) values did not differ between the three TRF groups, except for aspartate, β-alanine, and cis-aconitate (Figure 4C–E; Figure S1, $p < .05$ and VIP score >1.8 for all three metabolites; ANOVA). This indicates that the alterations in metabolite rhythms mostly result from shifts in the peak phase and not from strongly increased or decreased levels of the metabolites at a certain timepoint (which can also induce/abolish rhythmicity).

We used MetaboAnalyst to compare differences in rhythmic metabolite sets between the light- and dark-fed animals (i.e., the metabolites that were rhythmic in only one of these two groups). The top 6 highest metabolite enrichment set results were (in order of significance): Warburg effect, Purine metabolism, pentose phosphate pathway (PPP), pyrimidine metabolism, TCA-cycle, and gluconeogenesis (all *p*-values <.005; all false-discovery-rates (FDR) <0.1; Table S5).

3.4.2 | TRF leads to distinct lipid signatures

In addition to the polar metabolomics, nonpolar lipidomics was performed on the *soleus* muscle tissue during which >1000 lipid species could be identified and assessed for their rhythmicity. Light-fed animals had almost double

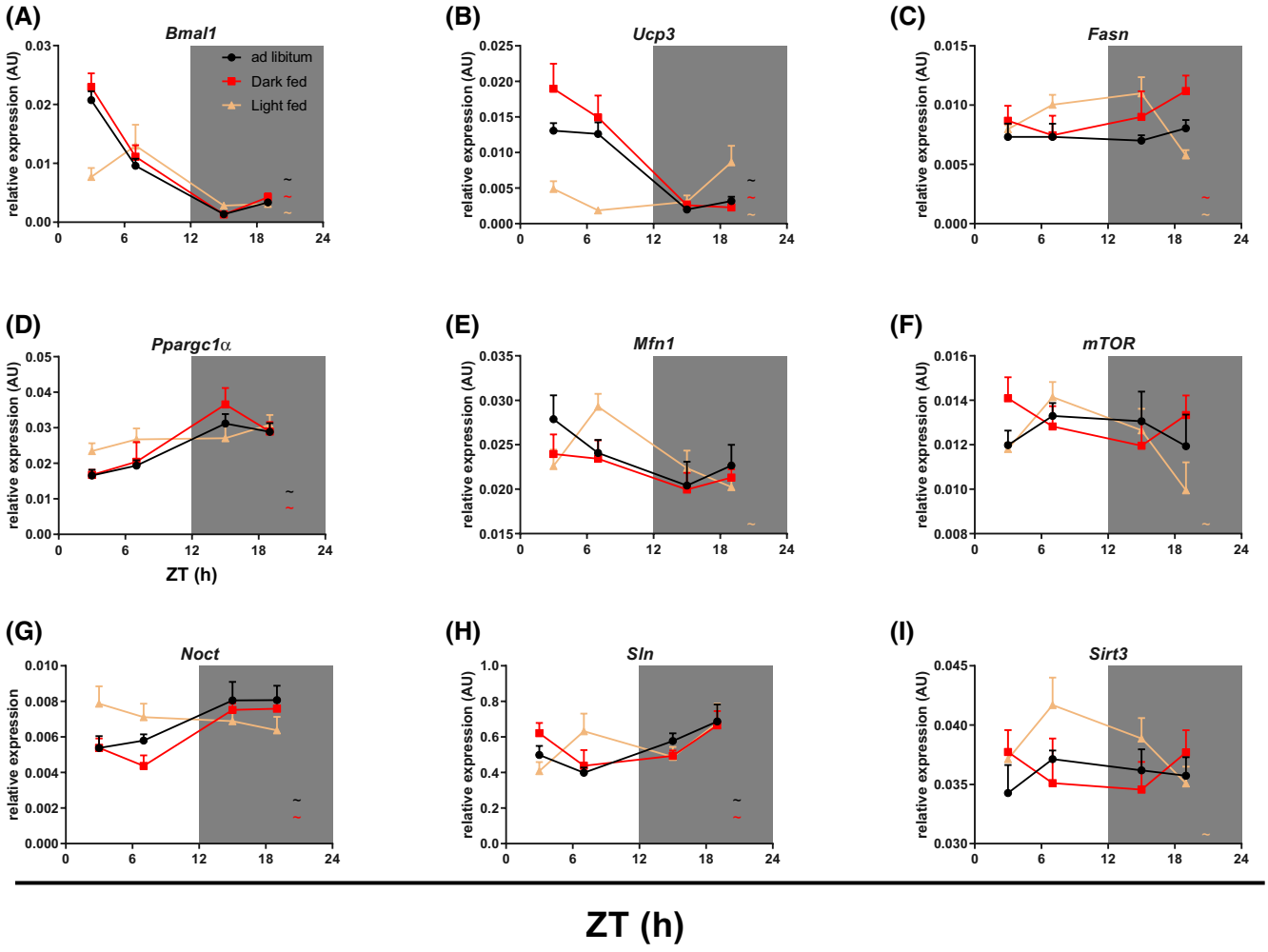

FIGURE 3 (A–L) Daily profiles of (mitochondrial) mRNA expression in the *soleus* muscle of the 3 experimental groups (a selection of 9 out of 18 tested genes). Table S1 lists the full name of all genes. Table S2 and Table S3 summarize the main statistical findings from respectively the 2 way ANOVA and JTK_Cycle analysis of all tested genes. Color-coded "~" indicates that the gene expression is significantly rhythmic for that TRF group as determined by JTK_Cycle ($p < .05$)

the number of intracellular skeletal muscle lipid species that showed significant rhythmicity as compared to AL and dark-fed animals (20%, 11%, and 12% of 1088 annotated lipid species, respectively) (Figure 5A and Table S6). Only five lipid species significantly fluctuated throughout the day in all three TRF groups: three bis(monoacylglycerol) phosphates (BMPs), i.e., BMP(38:5), BMP(38:6), and BMP(38:7), totaling 10% of all identified BMPs, lysophosphatidylcholine (LPC; 24:4), and lysophosphatidylethanolamine (LPE;O-17:1).

When assessing the individual lipid species within each specific class more closely, we found striking differences in the proportion of significantly rhythmic lipid species between the TRF groups (Figure 5A, Table S6). For example, in dark-fed animals, 48 out of 69 ether lipid (TG(O)) species were significantly rhythmic, while three species were rhythmic in light-fed animals, and none in the AL group (Figure 5A,C). In stark contrast, from the regular TG species, only one out of 259 species was significantly rhythmic in dark-fed animals, while in AL and light-fed animals 45 and 115 of the regular TG species were rhythmic, respectively.

We found no clear differences in the timing of the lipid rhythmicity that could be attributed to altered TRF feeding behavior (Figure 5 and Figure S2), except for triglycerides for which the average acrophase was ZT13.3 in AL animals, versus ZT10.5 for light-fed animals (Figure 5C), and for PI (AL average acrophase at ZT18.8; dark-fed average acrophase at ZT7.3; Figure S2).

Overall, daily (i.e., 24h average) values of lipids also differed between the TRF groups, with for example 14 different TG ether lipid species being higher in LF animals (20% of all TG(O) species measured) and three BMP species being lower in LF animals (10%) as compared to dark-fed animals (Table S7). Compared to the AL group, DF animals had higher overall levels of, for example, Cer

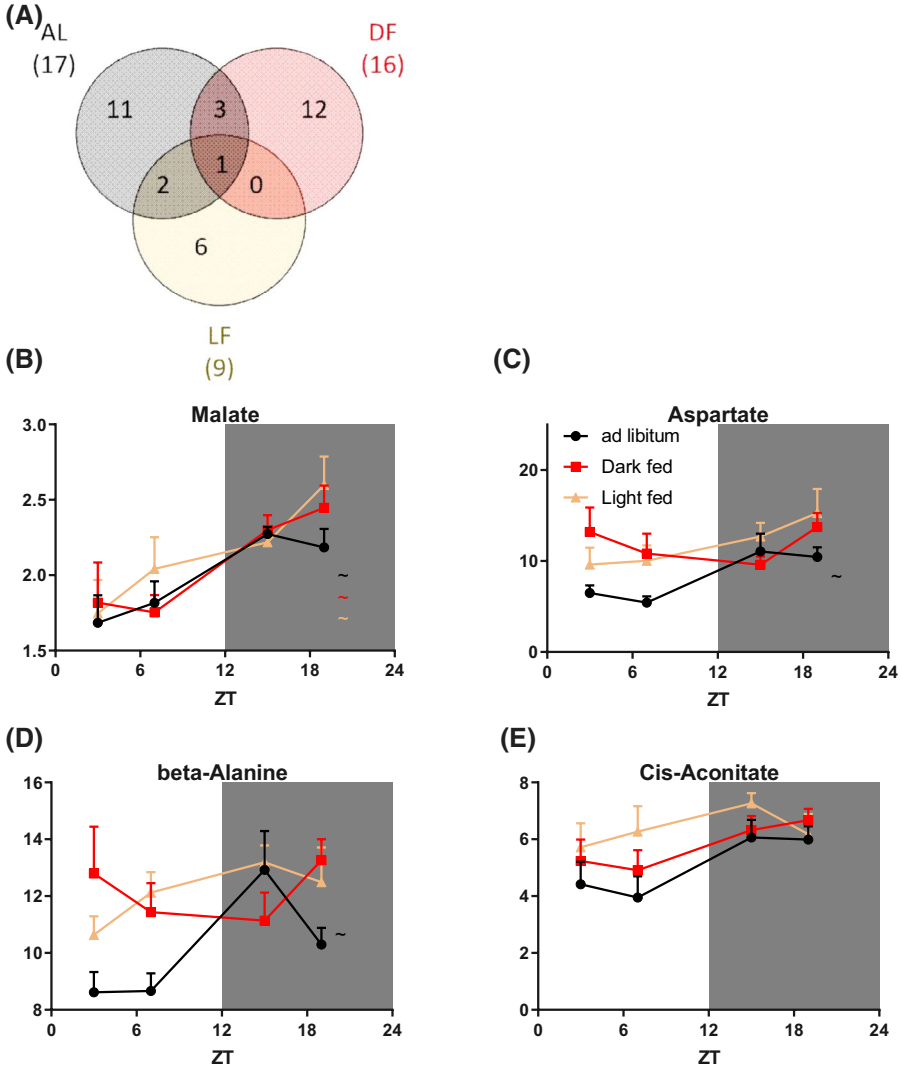

FIGURE 4 Metabolomics overview. (A) Venn diagram showing the total number of rhythmic polar metabolites out of the 97 tested, as well as the overlap in rhythmic metabolites for the 3 experimental groups. (B–E) Daily profiles of some of the polar metabolite levels in the *soleus* muscle of the 3 experimental groups. Depicted are malate (B; the only metabolite rhythmic in all TRF groups) and the three metabolites that showed a significant difference between groups in their 24 h-mean levels (C–E), that is, lower levels in the *ad libitum* group. Color-coded "~" indicates that a metabolite has significantly rhythmic abundance levels for that TRF group as determined by JTK_Cycle ($p < .05$)

(six species, 18%), LPC (five species, 12%), and TG(O) (one species, 20%), but lower levels for two lipid classes: BMP (one species, 3%) and CL (one species, 20%). Compared to the AL group light-fed animals had higher overall levels of 3 DG species (3%), 4 DG(O) species (19%), and 13 TG(O) species (19%) and lower levels for a single TG species only.

To zoom in on the muscle lipid species that are under the control of the circadian timing system we eliminated the influence of feeding status by comparing only the time points at which the light-fed and dark-fed animals just had obtained access to their food (Figure S3; i.e., *Just-Ate*, which is ZT3 for the light-fed and ZT15 for the dark-fed animals) or when they both had been fasting for 14 h (i.e., *Hungry*, which is ZT19 for the light-fed animals and ZT7 for the Dark-fed animals). With this analysis, we found some remarkable differences between LF and DF animals, which are thus independent of feeding status. For instance, in the *Just-Ate* condition, LF animals had higher levels of two ether lipid LPE species (22% of total LPE(O) species), but lower levels of ten BMP species (34%) and 96 TG species (37%) (Table S8). Conversely, in the *Hungry* condition LF animals had lower levels of one ether lipid LPE species (11%), but higher levels of nine BMP species (31%).

4 | DISCUSSION

The current data provide clear evidence for significant daily rhythmicity in rat muscle maximal ex vivo mitochondrial respiration. TRF to the dark/active phase (i.e., aligned with the circadian timing system) strengthened this daily rhythm in mitochondrial metabolism, whereas feeding restricted to the inactive phase strongly dampened the amplitude of this rhythm and reduced the overall 24-h respiration rate. Analysis of mitochondrial abundance, activity, and gene expression indicated a possible role for the mitochondrial biogenesis and fission/fusion machinery. Metabolomics demonstrated a multitude of rhythmic metabolites of especially intermediates of the pentose phosphate pathway and the TCA cycle in AL and dark-fed

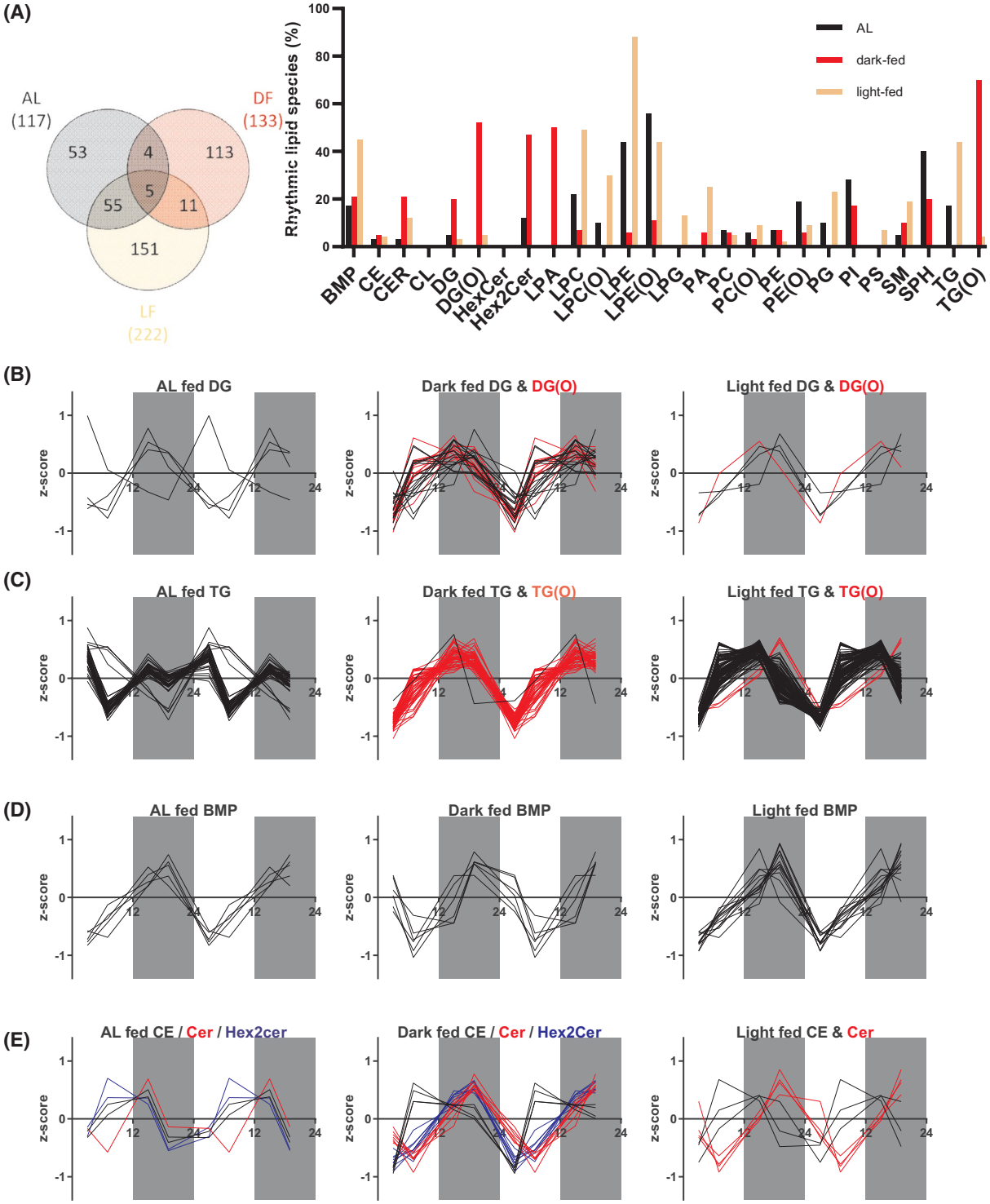

FIGURE 5 Lipidomics overview. (A) (left) Venn diagram showing the total number of rhythmic lipids, as well as the overlap in rhythmic lipids for the 3 experimental groups; (right) Histogram displaying the percentage of lipid species that were significantly rhythmic for each experimental group, sorted per main lipid class. (B–E) Daily profiles of lipid levels in the *soleus* muscle of the 3 experimental groups. Depicted are the z-transformed data of all lipid species that were significantly rhythmic, sorted per main lipid class. Data are double-plotted for easier visual inspection, however, statistics were performed on the single-plotted data. See Figure S2 for the daily profiles of the remaining main lipid classes. (F) Polar plots depicting when the different lipid species have their peak abundance levels during the L/D cycle for each of the TRF groups. The different lipid classes are color-coded according to the legend to the right. Numbers on the outer edge of the circle refer to the time of day for peak abundance levels of the lipid species. Sizes of the colored parts indicate how many lipid species peaked during that time of day (i.e., the further away from the origin of the circle the more lipid species peaked during that time of day)

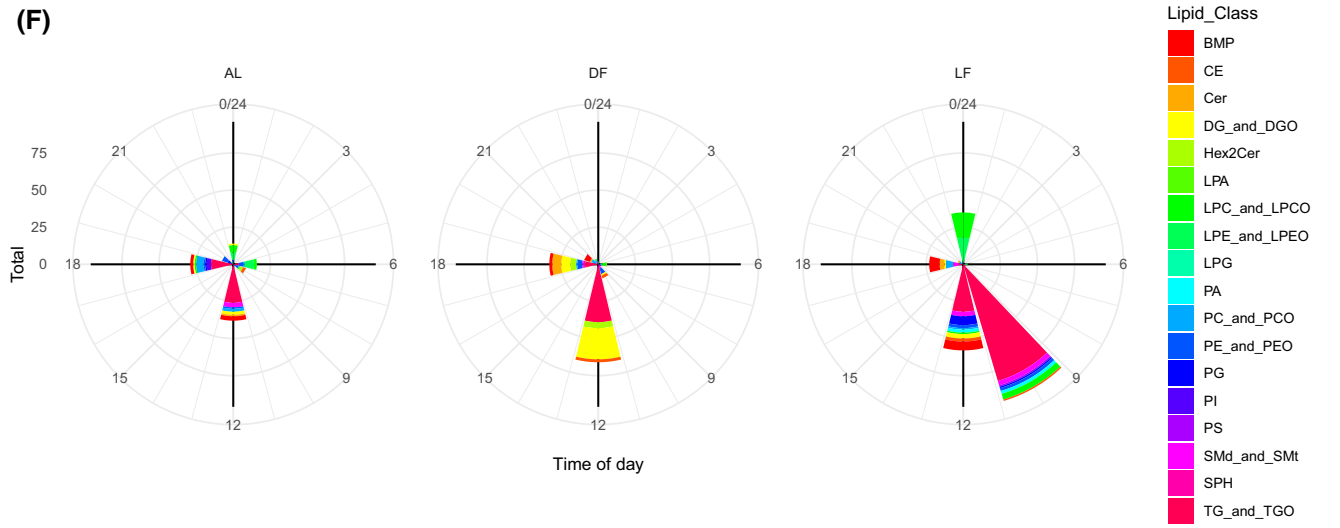

FIGURE 5 (Continued)

animals, but no daily rhythms in light-fed animals were found for these pathways. Contrastingly, lipidomics showed that light-fed animals abundantly gained rhythmicity in levels of triglycerides. Bis(monoacylglycero) phosphate and both diglycerides and ether triglycerides were the most affected lipid species.

4.1 | Rhythmicity of skeletal muscle mitochondrial respiration

Our results confirm that clear daily rhythms in mitochondrial respiration exist in permeabilized muscle fibers, which is in agreement with other small animal studies[40-44] and in vitro approaches.[45-49] A recent study in healthy humans observed a similar difference between the highest and lowest daily respiration rate (20% vs. 18% in this study).[27] In that study, no rhythmicity in maximal uncoupled respiration was found, but this is likely due to the large inter-person variation.[27] In both studies, the daily peak in OXPHOS capacity was not in the active phase (daytime in humans, nighttime in rats), but rather in the inactive phase (11:00 p.m. in humans, ZT6 in our study). The underlying cause of the higher maximal OXPHOS capacity during the inactive phase is currently unknown. Furthermore, we observed that the overall maximal OXPHOS capacity was 11% lower in the light-fed group (i.e., our circadian misalignment group), which is quite similar to the 14% difference observed when comparing humans in an acute circadian aligned and misaligned shift-work protocol.[50] Therefore, disturbing the circadian system, such as occurs during shift-work, could be causal or at least contribute significantly to the pathology of T2DM.

An important observation was that the total mitochondrial abundance and activity (assessed by mtDNA/nDNA and citrate synthase activity) was not different across the day in AL and dark-fed animals, indicating that the cause of this daily rhythmicity likely resides in mitochondrial proteostasis or other factors of mitochondrial quality such as mitochondrial dynamics. Surprisingly, in the light-fed group mitochondrial abundance appeared to be rhythmic. We think that feeding during the inactive phase disturbs the balance in mitochondrial biogenesis, mitophagy, and fission/fusion, resulting in abnormal mitochondrial abundance patterns throughout the day. Several studies have indeed provided evidence for daily rhythms in mitochondrial dynamics.[27,46,50,51,52] To further provide mechanistic insight into the reason for the lower respiration and dampened rhythmicity in the light-fed animals, we analyzed gene expression profiles of several important mitochondrial genes.

We found several mitochondria-related genes that lost their rhythmic expression in the light-fed group, such as *Ppargc1a*, *Sln*, and *Noct*, while others gained rhythmic expression (*Mfn1*, *mTOR*, and *Sirt3*). The dysregulation that we found in the expression of these genes thus fits well with the idea of circadian disruption of mitochondrial functioning through daytime TRF.

However, most mitochondria-related genes tested showed no rhythmic expression and thus the effect of TRF on rhythmicity could not be assessed. This is not surprising as only an estimated 4% of all transcripts are rhythmic in mice skeletal muscle.[3]

4.2 | Rhythmicity of skeletal muscle metabolite and lipid concentrations

Using the same *soleus* muscle tissue for both polar metabolomics as well as lipidomics, we were able to get a better understanding of the individual metabolites affected by

TRF. The polar metabolomics showed profound changes in some of the major muscle metabolic pathways as a result of TRF, such as the TCA cycle, glycolysis, and the pentose phosphate pathway, both in light-fed and dark-fed animals. More specifically, although the total number of rhythmic metabolites remained unaltered, the muscle tissue of dark-fed animals showed an enrichment of PPP metabolites as compared to AL feeding. Conversely, TRF during the inactive phase showed a quite drastic change in the pool of rhythmic metabolites, with a roughly halving and doubling of rhythmic polar metabolites and lipids, respectively. Additionally, various alterations in the types of metabolites that were rhythmic were observed in these light-fed animals, such as a strong reduction in the number of rhythmic TCA cycle and glycolysis intermediates. Furthermore, a gain of rhythm in the muscle waste products creatinine and lactate was observed. One explanation for the latter findings is that maximal OXPHOS capacity is reduced in light-fed animals, especially during the light phase, while during this period the activity of the animals is higher. Therefore, during the light phase, the ATP demand is increased while OXPHOS is decreased, likely resulting in an increase in alternative metabolic pathways such as (anaerobic) glycolysis and creatine metabolism and thus altered levels of creatinine and lactate. Adding to this notion is the increased RER of light-fed animals during the light phase, as also observed previously,[35,37,38] which supports the notion of increased lactate production through glycolysis. Taken together these findings suggest that eating at the wrong time disrupts metabolic flexibility in skeletal muscle which can contribute to pathological conditions such as T2DM (reviewed in Ref. [53]).

When looking at peak abundance of the different lipid species it becomes clear that the peak time of most rhythmic lipid species clusters in the dark phase for all three TRF groups (Figure 5B–E and Figure S2). When averaging the acrophases of all significantly rhythmic lipids only small shifts are found for the dark-fed compared to the light-fed animals. This indicates that these rhythms are not driven by the timing of food intake, but are mostly determined by the circadian timing system. Especially in the light-fed group, much larger shifts would be expected when the timing of food intake would determine the phasing of these rhythms. The fact that these rhythms are not adjusted upon TRF implies a consequent imbalance between energy supply and demand for light-fed animals. Regardless of its timing, TRF clearly induces an unique muscle lipid signature for both regular and ether TGs. A similar conclusion was recently drawn by Mehus et al. for the effects of TRF on the liver of mice fed a high-fat diet.[54] Since increased TG levels are known to interfere with the functioning of the main insulin-dependent glucose transporter GLUT4, the disturbances in TG metabolism in the light-fed group provide a possible mechanism for the disturbed glucose metabolism found in our shift-work model.[55] For ether lipid DGs something similar was observed regarding rhythmicity, with dark-fed animals having 52% of the DG(O) lipid species showing significant fluctuations throughout the day, but in light-fed and AL animals these figures were only 5% and 0%, respectively. The specific functions of most of these lipid species remain to be investigated, as well as the mechanisms responsible for these large changes in abundance.

BMPs are negatively charged glycerophospholipids that are considered important for nutrient cycling through lysosomal activity.[56] The role of BMPs in skeletal muscle is not well studied, but BMPs are known to be affected by feeding status with lowered levels in skeletal muscle within 2 h of refeeding fasted mice,[56] which fits with the changes in 24h mean levels induced by TRF (Figure 5, Tables S6–S8). In addition, our data indicate that BMPs in skeletal muscle are likely also under the control of the biological clock. Strikingly, whereas only five out of the 1088 annotated lipids showed a significant rhythm in all three experimental groups, three of those were BMPs. Intriguingly, the percentage of annotated BMPs that showed a significant rhythm more than doubled in the light-fed group (45% of all 29 identified BMPs) as compared to both AL and dark-fed animals, while light-fed animals overall had lower BMP levels as compared to dark-fed animals. Future studies should elucidate the exact roles of lipids such as DG(O)s, TG(O)s, and BMPs in the regulation of daily metabolism in skeletal muscle. Finally, our finding that ~11% of all measured lipids are rhythmic matches closely the finding that 13% of measured lipids in the human *vastus lateralis* display rhythmicity and thus adds to the validity of our animal model.[57]

Concluding, we report the presence of a daily rhythm in mitochondrial respiration in skeletal muscle in rats. The amplitude of this daily rhythm in respiration was enhanced by restricting food intake to the active phase. Contrasting, eating at the wrong time of day, as is often the case during shift work, abolished the rhythm in mitochondrial respiration. Moreover, 24-h respiration levels were significantly decreased in the misaligned animals, an observation that parallels the reduced oxidative capacity observed previously in T2DM patients. Metabolomics and lipidomics indicated that these misaligned animals had lost a rhythmic abundance of α-ketoglutarate and citric acid levels, while triglyceride levels gained rhythmicity. Furthermore, due to the significant influence of the circadian timing system many measured metabolic parameters (e.g., activity and mitochondrial respiration) did not strictly align with the shifted timing of food intake, resulting in a mismatch between expected metabolic supply/demand (as dictated by the circadian timing system and

L/D cycle) and the actual metabolic supply/demand (as dictated by the timing of food intake and locomotor activity). Adding to this are the observations that the RER did shift entirely while peak timing of most lipid classes assessed did not shift at all with the altered feeding behavior.

In this regard, it is unfortunate that with the current experimental set-up it is not possible to completely separate the effects of the L/D cycle and timing of food intake. Ideally, these experiments should also be performed in dark/dark conditions, with food restricted to either the subjective day or subjective night. However, the free-running rhythms that will be initiated in these constant conditions make this a challenging experimental design, i.e., the timing of the access to food will have to be adapted every day for every individual animal. Interestingly, recently, Heyde & Oster[58] used another experimental design to approach this question. They exposed their animals to a combined 28-h L/D cycle and a 24-h feeding/fasting cycle, or the other way around, to separate the effects of the L/D cycle and feeding time. Liver and adipose tissue exhibited the strongest correlation with the feeding cycle, whereas the SCN and adrenal gland showed a stronger influence by light.

Taken together, these findings indicate that shift-work impairs muscle mitochondrial functioning on multiple levels, which eventually could lead to metabolic disorders such as T2DM. Thus, our results suggest that mitochondria are an interesting therapeutic target for the prevention or even treatment of T2DM as they can be targeted not only by pharmaceutical drugs, but can also be influenced by lifestyle interventions. Examples of such lifestyle interventions are dietary interventions (both caloric restriction as well as nutritional supplements such as resveratrol, carnitine, and NAD^+ precursors) and (timed) exercise and other measures to strengthen circadian rhythms. Therefore, these interventions urgently need further confirmation in human studies in the context of treatment and/or prevention of T2DM,[11] especially whether an optimized combination and timing of exercise and diet can further enhance their separate effects.

ACKNOWLEDGEMENT

P. de Goede was funded by a ZonMW TOP grant (#91214047).

DISCLOSURES

The authors have stated explicitly that there are no conflicts of interest in connection with this article.

AUTHOR CONTRIBUTIONS

Paul de Goede, Andries Kalsbeek and Riekelt H. Houtkooper designed research. Paul de Goede, Rob C. I. Wüst, Bauke V. Schomakers and Simone Denis performed research. Paul de Goede, Rob C. I. Wüst, Bauke V. Schomakers, Frédéric M. Vaz, Mia L. Pras-Raves and Michel van Weeghel analyzed data. Paul de Goede, Rob C. I. Wüst, Chun-Xia Yi, Andries Kalsbeek and Riekelt H. Houtkooper wrote the paper. All other read, edited and approved the manuscript.

ORCID

Paul de Goede https://orcid.org/0000-0003-4489-7422
Andries Kalsbeek https://orcid.org/0000-0001-9606-8453

REFERENCES

1. Krishnaiah SY, Wu G, Altman BJ, et al. Clock regulation of metabolites reveals coupling between transcription and metabolism. *Cell Metab*. 2017;25(4):961-974.e4. doi:10.1016/j.cmet.2017.03.019
2. Bailey SM, Udoh US, Young ME. Circadian regulation of metabolism. *J Endocrinol*. 2014;222(2):R75-R96. doi:10.1530/JOE-14-0200
3. Zhang R, Lahens NF, Ballance HI, Hughes ME, Hogenesch JB. A circadian gene expression atlas in mammals: implications for biology and medicine. *Proc Natl Acad Sci U S A*. 2014;111(45):16219-16224. doi:10.1073/pnas.1408886111
4. Pan A, Schernhammer ES, Sun Q, Hu FB. Rotating night shift work and risk of type 2 diabetes: two prospective cohort studies in women. *PLoS Med*. 2011;8(12):e1001141. doi:10.1371/journal.pmed.1001141
5. Vetter C, Dashti HS, Lane JM, et al. Night shift work, genetic risk, and type 2 diabetes in the UK biobank. *Diabetes Care*. 2018;41(4):762-769. doi:10.2337/dc17-1933
6. Knutsson A, Kempe A. Shift work and diabetes—a systematic review. *Chronobiol Int*. 2014;31(10):1146-1151. doi:10.3109/07420528.2014.957308
7. Schrauwen P, Hesselink MKC. Oxidative capacity, lipotoxicity, and mitochondrial damage in type 2 diabetes. *Diabetes*. 2004;53(6):1412-1417. doi:10.2337/diabetes.53.6.1412
8. Kwak SH, Park KS, Lee K-U, Lee HK. Mitochondrial metabolism and diabetes. *J Diabetes Investig*. 2010;1(5):161-169. doi:10.1111/j.2040-1124.2010.00047.x
9. Sivitz WI, Yorek MA. Mitochondrial dysfunction in diabetes: from molecular mechanisms to functional significance and therapeutic opportunities. *Antioxid Redox Signal*. 2010;12(4):537-577. doi:10.1089/ars.2009.2531
10. Fujimaki S, Kuwabara T. Diabetes-induced dysfunction of mitochondria and stem cells in skeletal muscle and the nervous system. *Int J Mol Sci*. 2017;18(10):2147. doi:10.3390/ijms18102147
11. Hesselink MKC, Schrauwen-Hinderling V, Schrauwen P. Skeletal muscle mitochondria as a target to prevent or treat type 2 diabetes mellitus. *Nat Rev Endocrinol*. 2016;12(11):633-645. doi:10.1038/nrendo.2016.104
12. Montgomery MK, Turner N. Mitochondrial dysfunction and insulin resistance: an update. *Endocr Connect*. 2015;4(1):R1-R15. doi:10.1530/EC-14-0092
13. Gordon JW, Dolinsky VW, Mughal W, Gordon GRJ, McGavock J. Targeting skeletal muscle mitochondria to prevent type 2 diabetes in youth. *Biochem Cell Biol*. 2015;93(5):452-465. doi:10.1139/bcb-2015-0012

14. He J, Watkins S, Kelley DE. Skeletal muscle lipid content and oxidative enzyme activity in relation to muscle fiber type in type 2 diabetes and obesity. *Diabetes*. 2001;50(4):817-823. doi:10.2337/diabetes.50.4.817
15. Kelley DE, He J, Menshikova EV, Ritov VB. Dysfunction of mitochondria in human skeletal muscle in type 2 diabetes. *Diabetes*. 2002;51(10):2944-2950.
16. Petersen KF, Befroy D, Dufour S, et al. Mitochondrial dysfunction in the elderly: possible role in insulin resistance. *Science*. 2003;300(5622):1140-1142. doi:10.1126/science.1082889
17. Phielix E, Schrauwen-Hinderling VB, Mensink M, et al. Lower intrinsic ADP-stimulated mitochondrial respiration underlies in vivo mitochondrial dysfunction in muscle of male type 2 diabetic patients. *Diabetes*. 2008;57(11):2943-2949. doi:10.2337/db08-0391
18. Phielix E, Meex R, Moonen-Kornips E, Hesselink MKC, Schrauwen P. Exercise training increases mitochondrial content and ex vivo mitochondrial function similarly in patients with type 2 diabetes and in control individuals. *Diabetologia*. 2010;53(8):1714-1721. doi:10.1007/s00125-010-1764-2
19. Deshmukh AS. Insulin-stimulated glucose uptake in healthy and insulin-resistant skeletal muscle. *Horm Mol Biol Clin Investig*. 2016;26(1):13-24. doi:10.1515/hmbci-2015-0041
20. Honka M-J, Latva-Rasku A, Bucci M, et al. Insulin-stimulated glucose uptake in skeletal muscle, adipose tissue and liver: a positron emission tomography study. *Eur J Endocrinol*. 2018;178(5):523-531. doi:10.1530/EJE-17-0882
21. Hoppeler H, Flück M. Normal mammalian skeletal muscle and its phenotypic plasticity. *J Exp Biol*. 2002;205(Pt 15):2143-2152.
22. Harfmann BD, Schroder EA, Esser KA. Circadian rhythms, the molecular clock, and skeletal muscle. *J Biol Rhythms*. 2014;30(2):84-94. doi:10.1177/0748730414561638
23. Perrin L, Loizides-Mangold U, Chanon S, et al. Transcriptomic analyses reveal rhythmic and CLOCK-driven pathways in human skeletal muscle. *Elife*. 2018;7:1-30. doi:10.7554/eLife.34114
24. McCarthy JJ, Andrews JL, McDearmon EL, et al. Identification of the circadian transcriptome in adult mouse skeletal muscle. *Physiol Genomics*. 2007;31(1):86-95. doi:10.1152/physiolgenomics.00066.2007
25. Hodge BA, Wen Y, Riley LA, et al. The endogenous molecular clock orchestrates the temporal separation of substrate metabolism in skeletal muscle. *Skelet Muscle*. 2015;5(1):17. doi:10.1186/s13395-015-0039-5
26. Dyar KA, Ciciliot S, Wright LE, et al. Muscle insulin sensitivity and glucose metabolism are controlled by the intrinsic muscle clock. *Mol Metab*. 2014;3(1):29-41. doi:10.1016/j.molmet.2013.10.005
27. van Moorsel D, Hansen J, Havekes B, et al. Demonstration of a day-night rhythm in human skeletal muscle oxidative capacity. *Mol Metab*. 2016;5(8):635-645. doi:10.1016/j.molmet.2016.06.012
28. Manella G, Asher G. The circadian nature of mitochondrial biology. *Front Endocrinol (Lausanne)*. 2016;7:8-11. doi:10.3389/fendo.2016.00162
29. Sardon Puig L, Valera-Alberni M, Cantó C, Pillon NJ. Circadian rhythms and mitochondria: connecting the dots. *Front Genet*. 2018;9:1-8. doi:10.3389/fgene.2018.00452
30. de Goede P, Wefers J, Brombacher EC, Schrauwen P, Kalsbeek A. Circadian rhythms in mitochondrial respiration. *J Mol Endocrinol*. 2018;60(3):R115-R130. doi:10.1530/JME-17-0196
31. Wüst RCI, Myers DS, Stones R, et al. Regional skeletal muscle remodeling and mitochondrial dysfunction in right ventricular heart failure. *Am J Physiol Circ Physiol*. 2012;302(2):H402-H411. doi:10.1152/ajpheart.00653.2011
32. van den Berg M, Hooijman PE, Beishuizen A, et al. Diaphragm atrophy and weakness in the absence of mitochondrial dysfunction in the critically Ill. *Am J Respir Crit Care Med*. 2017;196(12):1544-1558. doi:10.1164/rccm.201703-0501OC
33. Shepherd D, Garland PB. 2] Citrate synthase from rat liver. [EC 4.1.3.7 citrate oxaloacetage-lyase (CoA-acetylating). *Methods Enzymol*. 1969;13(C):11-16. doi:10.1016/0076-6879(69)13006-2
34. Molenaars M, Schomakers BV, Elfrink HL, et al. Metabolomics and lipidomics in C. elegans using a single sample preparation. *bioRxiv*. 14(4):dmm047746. doi:10.1101/2020.07.06.190017
35. de Goede P, Sen S, Oosterman JE, et al. Differential effects of diet composition and timing of feeding behavior on rat brown adipose tissue and skeletal muscle peripheral clocks. *Neurobiol Sleep Circadian Rhythm*. 2018;4:24-33. doi:10.1016/j.nbscr.2017.09.002
36. de Goede P, Foppen E, Ritsema WIGR, Korpel NL, Yi C-X, Kalsbeek A. Time-restricted feeding improves glucose tolerance in rats, but only when in line with the circadian timing system. *Front Endocrinol (Lausanne)*. 2019;10:554. doi:10.3389/fendo.2019.00554
37. de Goede P, Hellings TP, Coopmans TV, Ritsema WIGR, Kalsbeek A. After-effects of time-restricted feeding on whole-body metabolism and gene expression in four different peripheral tissues. *Obesity*. 2020;28(S1):S68-S80. doi:10.1002/oby.22830
38. Opperhuizen A-L, Wang D, Foppen E, et al. Feeding during the resting phase causes profound changes in physiology and desynchronization between liver and muscle rhythms of rats. *Eur J Neurosci*. 2016;44(10):2795-2806. doi:10.1111/ejn.13377
39. Oosterman JE, Koekkoek LL, Foppen E, et al. Synergistic effect of feeding time and diet on hepatic steatosis and gene expression in male wistar rats. *Obesity*. 2020;28(S1). doi:10.1002/oby.22832
40. Andrews JL, Zhang X, McCarthy JJ, et al. CLOCK and BMAL1 regulate MyoD and are necessary for maintenance of skeletal muscle phenotype and function. *Proc Natl Acad Sci U S A*. 2010;107(44):19090-19095. doi:10.1073/pnas.1014523107
41. Woldt E, Sebti Y, Solt LA, et al. Rev-erb-α modulates skeletal muscle oxidative capacity by regulating mitochondrial biogenesis and autophagy. *Nat Med*. 2013;19(8):1039-1046. doi:10.1038/nm.3213
42. Jordan SD, Kriebs A, Vaughan M, et al. CRY1/2 selectively represses PPARδ and limit exercise capacity. *Cell Metab*. 2017;26(1):243-255.e6. doi:10.1016/j.cmet.2017.06.002
43. Bray MS, Shaw CA, Moore MWS, et al. Disruption of the circadian clock within the cardiomyocyte influences myocardial contractile function, metabolism, and gene expression. *AJP Hear Circ Physiol*. 2008;294(2):H1036-H1047. doi:10.1152/ajpheart.01291.2007
44. Cela O, Scrima R, Pazienza V, et al. Clock genes-dependent acetylation of complex I sets rhythmic activity of mitochondrial OxPhos. *Biochim Biophys Acta - Mol Cell Res*. 2016;1863(4):596-606. doi:10.1016/j.bbamcr.2015.12.018
45. Peek CB, Affinati AH, Ramsey KM, et al. Circadian clock NAD+ cycle drives mitochondrial oxidative metabolism in mice. *Science*. 2013;342(6158):1243417. doi:10.1126/science.1243417
46. Jacobi D, Liu S, Burkewitz K, et al. Hepatic Bmal1 regulates rhythmic mitochondrial dynamics and promotes

metabolic fitness. *Cell Metab*. 2015;22(4):709-720. doi:10.1016/j.cmet.2015.08.006

47. Simon N, Papa K, Vidal J, Boulamery A, Bruguerolle B. Circadian rhythms of oxidative phosphorylation: effects of rotenone and melatonin on isolated rat brain mitochondria. *Chronobiol Int*. 2003;20(3):451-461.
48. Scrima R, Cela O, Merla G, et al. Clock-genes and mitochondrial respiratory activity: evidence of a reciprocal interplay. *Biochim Biophys Acta - Bioenerg*. 2016;1857(8):1344-1351. doi:10.1016/j.bbabio.2016.03.035
49. Neufeld-Cohen A, Robles MS, Aviram R, et al. Circadian control of oscillations in mitochondrial rate-limiting enzymes and nutrient utilization by PERIOD proteins. *Proc Natl Acad Sci U S A*. 2016;113(12):E1673-E1682. doi:10.1073/pnas.1519650113
50. Wefers J, van Moorsel D, Hansen J, et al. Circadian misalignment induces fatty acid metabolism gene profiles and compromises insulin sensitivity in human skeletal muscle. *Proc Natl Acad Sci U S A*. 2018;115(30):7789-7794. doi:10.1073/pnas.1722295115
51. Oliva-Ramírez J, Moreno-Altamirano MMB, Pineda-Olvera B, Cauich-Sánchez P, Sánchez-García FJ. Crosstalk between circadian rhythmicity, mitochondrial dynamics and macrophage bactericidal activity. *Immunology*. 2014;143(3):490-497. doi:10.1111/imm.12329
52. Gong C, Li C, Qi X, et al. The daily rhythms of mitochondrial gene expression and oxidative stress regulation are altered by aging in the mouse liver. *Chronobiol Int*. 2015;32(9):1254-1263. doi:10.3109/07420528.2015.1085388
53. Smith RL, Soeters MR, Wüst RCI, Houtkooper RH. Metabolic flexibility as an adaptation to energy resources and requirements in health and disease. *Endocr Rev*. 2018;39(4):489-517. doi:10.1210/er.2017-00211
54. Mehus AA, Rust B, Idso JP, et al. Time-restricted feeding mice a high-fat diet induces a unique lipidomic profile. *J Nutr Biochem*. 2021;88:108531. doi:10.1016/j.jnutbio.2020.108531
55. Makrecka-Kuka M, Liepinsh E, Murray AJ, et al. Altered mitochondrial metabolism in the insulin-resistant heart. *Acta Physiol*. 2020;228(3):e13430. doi:10.1111/apha.13430
56. Grabner GF, Fawzy N, Schreiber R, et al. Metabolic regulation of the lysosomal cofactor bis(monoacylglycero)phosphate in mice. *J Lipid Res*. 2020;61(7):995. doi:10.1194/JLR.RA119000516
57. Held NM, Wefers J, van Weeghel M, et al. Skeletal muscle in healthy humans exhibits a day-night rhythm in lipid metabolism. *Mol Metab*. 2020;37:100989. doi:10.1016/j.molmet.2020.100989
58. Heyde I, Oster H. Differentiating external zeitgeber impact on peripheral circadian clock resetting. *Sci Rep*. 2019;9(1). doi:10.1038/s41598-019-56323-z.

SUPPORTING INFORMATION

Additional supporting information may be found in the online version of the article at the publisher's website.

How to cite this article: de Goede P, Wüst RCI, Schomakers BV, et al. Time-restricted feeding during the inactive phase abolishes the daily rhythm in mitochondrial respiration in rat skeletal muscle. *FASEB J*. 2022;36:e22133. doi:10.1096/fj.202100707R